Endocrinology

Modeling TSH Receptor Dimerization at the Transmembrane Domain

--Manuscript Draft--

Manuscript Number:	en.2022-00570R2
Full Title:	Modeling TSH Receptor Dimerization at the Transmembrane Domain
Article Type:	Research Article
Section/Category:	Thyroid
Corresponding Author:	Mihaly Mezei, PhD Icahn School of Medicine at Mount Sinai New York, UNITED STATES
Other Authors:	Rauf Latif
	Terry F Davies
Additional Information:	
Question	**Response**
DATA REPOSITORIES AND DATA REGISTRATION I have read and agree to take appropriate action to comply with the following Data Repositories and Data Registration guidelines and confirm that I have included the appropriate registration numbers / information in the text of the manuscript being submitted.	Not Applicable
CELL LINE AUTHENTICATION I have read and understood the Cell Line Authentication policy and describe my submission as follows:	Not applicable to my manuscript.
STEROID HORMONE MEASUREMENT I have read and understood the Steroid Hormone Measurement policy and describe my submission as follows:	Not applicable to my manuscript.

SPECIAL REQUESTS In place of a cover letter, you may enter specific comments or requests to the editors here.	
DATA AVAILABILITY The Endocrine Society requires that authors provide a statement about the availability of data generated or analyzed in the submitted manuscript. This statement will be included in the final version of accepted manuscripts. During the submission process, authors are asked to select a statement that best describes their data availability and to include the selected statement in the manuscript document, just before the reference list. This section of the manuscript should be labelled “Data Availability.” For more information, see the Author Guidelines. Options for these statements are below:	•Original data generated and analyzed during this study are included in this published article or in the data repositories listed in References.
Funding Information:	National Institute of Health (DK069713) — Terry F Davies U.S. Department of Veterans Affairs (BX000800) — Terry F Davies
Requested Editor:	
Author Comments:	TFD is member of the Board of Kronus Inc, Starr, Idaho; M.M. & R.L. have nothing to disclose.

Please **Note:** our answers to the reviewers' comments are in *italicized Times New Roman font* while the comments are in Calibri font. In the revised version added or changed text is colored red.

Editor Comments

Most of the reviewer comments have been considered in this revised manuscript. However, given the importance of the methods to the understanding of the results, the authors have not responded to several of the comments of reviewer 1 through the addition of some essential detail to the Methods, relying instead on reference to previous publications. The editor concurs with reviewer 1's original comments that additional detail should be added to the Methods, even if only 'in brief' summary form, so that readers are not required to reference external publications in order to understand the methods utilized in the current study.

The revised version now added further information requested by reviewer1. To be specific, we further addressed comments #1, #4, and #5. In our answers below we kept the original answer and added the description of actions taken in the current revision using ***bold italicized Times New Roman font.***

Reviewer Comments

Reviewer 1:

1. Line 55 states that after equilibrium, 600 ns of simulation were generated; nevertheless, the authors do not specify either the equilibration conditions nor those of the 600 ns of the MD to generate the TSHR-TMD-TRIO.

Original answer:

The details of the simulation leading to the TSHR-TMD-TRIO model have been described in a separate paper, reference #16. While we summarize here the major steps involved in setting up and performing the simulation, we think that it would be redundant to repeat all details of the simulation.

Current answer:

We added details of the equilibration protocol (established by the charm-gui server) and the conditions of the current simulation (ensemble, temperature, pressure, timestep). We also added a sentence each to describe the generic site concept and the TRAJELIX module.

4. Setup of the all-atom simulation was performed automatically with the charm-gui server. Nevertheless, given that the TSHR is a membrane protein, it is important to verify the stability of the membrane through evaluating the bilayer structure, including the area per lipid, the hydration level of the lipids, and the equilibration of the simulation box in x-, y-, and z- directions to verify the stability of its height, area, and other properties.

Original answer:

We have now added to the Result section a paragraph describing our monitoring of the stability of the system.

Current answer:

We added a statement saying that no lipid penetrated the dimer interface.

5. Residues of interaction between the TMD dimers should be verified by analyzing the effects of in silico mutations on dimer formation/stabilization.

Original answer:

The correctness of the dimer conformation was verified in the paper describing the Brownian dynamics calculations by mutating selected residues to cysteines and demonstrating that the resulting disulfide bonds covalently linked the two monomers.

Current answer:

We added a statement that discusses the crosslinking experiment.

Modeling TSH Receptor Dimerization at the Transmembrane Domain

Mihaly Mezei[1], Rauf Latif[2,3] and Terry F Davies[2,3.]

[1]Department of Pharmacological Sciences, [2]Thyroid Research Unit, Department of Medicine,

Icahn School of Medicine at Mount Sinai and

[3]James J. Peters VA Medical Center, New York, New York

ORCiD numbers: 0000-0003-0294-4307 (M. Mezei); 0000-0002-4226-3728 (R. Latif), 0000-0003-3909-2750 (T.F. Davies).

Running Title: TSH receptor dimers

Address correspondence to: Mihaly Mezei PhD. E-mail: mihaly.mezei@mssm.edu

Keywords: TSHR, GPCR, DPPC, molecular dynamics, dimerization, docking

Disclosure statement

TFD is member of the Board of Kronus Inc, Starr, Idaho; M.M. & R.L. have nothing to disclose.

Abbreviations: TSH – thyroid stimulating hormone, TSHR – TSH receptor, GPCR - G protein coupled receptor, Molecular Dynamics – MD

Abstract

Biophysical studies have established that the TSH receptor (TSHR) undergoes post translational modifications including dimerization. Following our earlier simulation of a TSH receptor – transmembrane domain (TMD) monomer (called TSHR-TMD-TRIO) we have now proceeded with a molecular dynamics simulation (MD) of TSHR-TMD dimerization using this improved membrane embedded model. The starting structure was the TMD protein with all extracellular and intracellular loops and internal waters, which was placed in the relative orientation of the model originally generated with Brownian dynamics. Furthermore, this model was embedded in a DPPC lipid bilayer, further solvated with water and added salt. Data from the molecular dynamic simulation studies showed that the dimeric subunits stayed in the same relative orientation and distance during the 1000 ns of study. Comparison of representative conformations of the individual monomers when dimerized with the conformations from the monomer simulation showed subtle differences as represented by the backbone RMSDs. Differences in the conformations of the ligand binding sites, suggesting variable affinities for these “hot spots”, were also revealed by comparing the docking scores of 46 small molecule ligands that included known TSHR agonists and antagonists as well as their derivatives. These data add further insight into the tendency of the TSHR-TMD to form dimeric and oligomeric structures and show that the differing conformations influence small molecule binding sites within the TMD.

INTRODUCTION

The TSH receptor (TSHR) is a class A GPCR with particular importance because of its involvement in autoimmune thyroid disease, particularly Graves' disease in which it is the primary antigen (1). The TSHR is a 764 amino acid protein comprising a large, heavily glycosylated, ectodomain (ECD) connected to a seven-helix transmembrane domain (TMD) via a hinge region (2,3). We have previously shown, by biochemical and biophysical methods that TSHRs in native, as well as transfected cells, exist as both dimeric and oligomeric units and that oligomerization may be regulated by exposure to the TSH ligand (3-5). Studies have also shown that TSHR dimerization may have physiological consequences including a role in receptor negative cooperativity (6) and G-protein selection and activation favoring Gαq (7). We have also shown previously that dimerization involves contact between the TSHR ECDs (8) and experimental data with truncated TSHRs have indicated that the TMD alone continues to dimerize and must also have a major role in TSHR dimerization and oligomerization (9).

Using a Brownian Dynamics approach (10) we previously generated a computer model for a TSHR dimer of the transmembrane domain (TMD) using our homology model (11). In this study the dimer model obtained was verified by mutating three pairs of residues forming contacts between the monomers to cysteines and verifying that this resulted in disulfide links between the monomers. Since then the TSHR-TMD monomer model has been further enhanced by generating its extracellular loops (12) by the Monte Carlo technique (13) and more recently, we used the same technique

to generate the intracellular loops. A grand-canonical ensemble (GCE) Monte Carlo (MC) simulation (14,15) was then used to add internal waters. This enhanced TSHR monomer model was subsequently embedded in a DPPC membrane including a water layer with counterions to neutralize the system and provide an environment with an ionic strength of 0.3 m/L. After equilibration, the membrane-embedded system was subjected to a 600 ns molecular dynamics (MD) simulation resulting in three representative structures of the TMD which we named TSHR-TMD-TRIO (16).

The improved membrane-embedded monomer model (TSHR-TMD-TRIO) has now allowed us to examine TSHR TMD dimerization with molecular dynamic simulation to gain better insight into receptor conformations and the interaction of allosteric ligands to the dimeric structure. The starting structure consisted of two copies of the initial TRIO protein with all loops and internal waters placed in the relative orientation of the model generated with Brownian dynamics which was embedded in a DPPC bilayer, further solvated with water, counter ions and added salt, as previously described (16).

MATERIALS AND METHODS

Initial TSHR TMD monomer model: The structure with the largest weight from the TSHR-TMD-TRIO structure (16) was used to prepare the initial dimer model. As for the generation of TSHR-TMD-TRIO, the positions of internal waters were obtained as generic sites (17) calculated with the program MMC (18). Generic sites are obtained in an iterative procedure where in each configuration waters are assigned to the current site estimates using a graph-theory based optimization.

Setting up for dimerization: Two copies of the TMD with the internal waters were arranged next to each other in a relative orientation that modeled the contacts established in our original dimer study (11). using a series of translations and rotations guided by the molecular graphics display (19). This dimer model with all loops generated and with internal water molecules in place was then sent to the charmm-gui server (20) to be inserted into a DPPC bilayer which also added the rest of the solvating waters and counterions. Besides the protein, the system contained 458 DPPC molecules, 97 K^+ ions, 121 Cl^- ions and 36,093 waters. The system generated used periodic boundary conditions with hexagonal prism as the unit cell. The initial height of the prism was 110 Å and the edge of the hexagon was 80 Å. The system thus generated included inputs for a six-step equilibration protocol and inputs for the production run(21), all using the program NAMD(22).

The equilibration protocol started with a 1000-step minimization, followed by MD simulations that imposed constraints on the protein, lipids and ions. Six simulations were performed with progressively weaker force constants; the sixth step released all constraints except for a very week constraint for the protein backbone. The first three runs were 125 ps long and used 1 fs timestep; the last three steps each were 500 ps long and used 2 fs timestep.

Dimer simulations: MD simulation was run using the program NAMD (22) in the (T,P,N) ensemble using 2 ps timestep. The temperature was set to 323.5 K, the pressure to 1 atm. The structures on the trajectory were clustered based on the

distances between the monomer backbone conformations represented as RMSD without the C-terminal tail. k-medoid clustering(23) was used separately for each monomer using the program Simulaid (24). This method uses as input the number of clusters requested and performs the clustering in an iterative manner without resorting to cutoffs; the number of clusters requested (three for both monomers) was arrived at observing the respective 2D RMSD matrix shown of Figure 3). For each cluster the conformation whose largest RMSD with the rest of the cluster members was the smallest among the members of the cluster was used as the representative structure to be used for docking. The analysis of the helix positions and orientations were performed with the TRAJELIX module (25) of the program Simulaid (24). TRAJELIX obtains the helix axis by fitting a line to the backbone atoms in residue ranges selected by the user; analyses are based on the coordinates of the beginning, middle and of the axes as well as on their direction.

Small molecule docking studies: The docking experiments described here used the program Glide (26,27) with the induced fit option. Before the docking runs the representative structures extracted from the MD run were subjected to minimization using the implicit membrane model GBMV (28). The minimization was set up with charmm-gui (20) and the minimization was run with Charmm (29). A set of 46 ligands were docked to each representative structure (**Supplementary Table 1**(30)). Among the ligands docked were active agonists (n=3) and antagonists (n=3) of variable potency, including ones developed in our laboratory (31), and derivatives of known active compounds (n=40). Not all derivatives, however, were found to be active.

Statistical evaluations: The tests for the significance of differences between score averages were performed with the Graphpad server (URL: https://www.graphpad.com/quickcalcs/ttest2/) using the two tailed Welch t-test that does not require the two samples to have the same variance.

RESULTS:

The TSHR monomer and initial dimer

Figure 1a illustrates a TSHR monomer extracted from the TSHR-TMD-TRIO model previously detailed (16) which was embedded in a lipid membrane. Important points to note include the conformation which was obtained from the MD simulation studies. The starting dimer conformation (**Figures 1b and 1c**) was derived by placing two copies of the monomer in an orientation suggested by our earlier Brownian Dynamic studies (11) and included the internal waters generated by the grand-canonical ensemble (GCE) MC simulation. The dimer interface constructed as described involved helices 1, 2 and 4 on monomer 1 (green) and helices 4 and 5 on monomer 2 (orange). This model conformation was then sent to the charmm-gui server.

MD simulation

The six-step equilibration protocol provided by the charmm-gui server was followed by a 1,000 nanosecond (ns) MD run using 2fs time step. The animation of the trajectory showed that the monomers stayed in contact throughout the simulation and no lipid molecules entered the interface. **Figure 2** shows the history of the many residue pairs in contact for more than 40% of the simulation time and making up the dimeric structure. Note that two atoms were considered to be in contact if they were mutually proximal (32). These data showed that the contact between monomers was maintained at all times throughout the simulation. There was no breakup of the dimeric conformation during the entire period of simulation.

The simulation box size during the simulation was monitored and was found stable. The simulation trajectory was also animated on a graphical display and no anomaly was observed in the bilayer; the counterions were found to sample well the solvent region and no significant water penetration was observed into the lipid bilayer nor was any lipid seen penetrating the dimer interface.

Dimer clustering

We then analyzed the structures by examining the clustering of the monomers in the dimer simulations. Clustering of similar monomer structures was found to be best represented by three dominant conformations for both monomers. These clusters were based on the backbone root mean square deviation (RMSD) calculated without the C-terminal tail.

The RMSD matrix of the conformations rearranged by clusters is shown in **Figures 3a and 3b** for monomers 1 and 2, respectively. The black lines delineate the different clusters. The cluster memberships are shown in **Figures 4a and 4b** for monomers 1 and 2, respectively showing that the monomer conformations were not totally consistent with time indicating movement between the clusters. Such movements are indicators of extensive sampling.

The overall conformations of the representative structures from the earlier TRIO model and the two simulated monomers were then compared by calculating the backbone RMSDs (with three representative structures from the clustering) for both of the newly simulated monomers (1 and 2) and the TRIO monomer making nine structures to analyze. The larger the RMSD the more flexible the structure is within the model. The matrix of the RMSDs is given in **Table 1** and shows that this type of analysis illustrates differences between the model structures; for example monomer 2 appears more flexible than monomer 1 and both show subtle differences between each other and from the TRIO monomer.

Intramolecular hydrogen bonding

The formation and breakup of the hydrogen bonds within the TMD monomers were compared for the 600 ns TRIO simulation and the two monomers within the 1000 ns dimer simulation by tracking the presence and absence of hydrogen bonds among all pairs of residues. **Figure 5** shows a typical graph for the second monomer of the dimer; residue pairs should be hydrogen bonded at least 20% of the time. Also, residues in the pair have to be at least five residues apart – this

eliminates the trivially present hydrogen bonds forming the transmembrane helices. **Supplementary Table 2**(30) lists the residue pairs that are hydrogen bonded according to the criteria above in at least one of the three models, the % of time they are hydrogen bonded and their multiplicity (1/2/3). Eleven residue pairs were hydrogen bonded in all three systems (**Table 2**) and their conservation indicated they likely represented important bonding sites.

Helix changes

As all GPCRs, the TMD of the TSHR consists of seven transmembrane helices. It also has an 8^{th} helix on the intracellular side and a long C-terminal tail. Helices 6 contains one proline and helix 7 contains two. Since prolines introduce kinks in helices, for the purpose of these analyses these two helices are broken into two (the short helix between the two prolines in helix 7 is ignored). The analyses described below for each property calculated its average over the three representative structure of one of the monomers and compared it with the corresponding value from the third structure in the TRIO model. If the value of the TRIO model fell outside the range of the monomer values then the change was considered significand (marked with 'S' in the respective table). The changes in the lengths (end-to end distance) of the transmembrane helices and the changes in the radii of the circle fitted to the helix axes (a measuring the degree of bent) are shown in **Table 3** for both monomers. Interestingly, most of the changes, while small, occur in a different direction for the two monomers. **Supplementary Table 3**(30) shows the changes in the helix-helix distances using two different

measures: the distance between the helix centers and the distance (closest approach) of the helix axes for monomers 1 and 2. For monomer 1, Helix 7 shows large changes while for Monomer 2 Helices 5 and 6 is seen the most variable and **Supplementary Table 4**(30) contains the changes in the helix-helix angles. They display similar behavior as the distances: for monomer 1 Helix 7 shows the largest changes while for monomer 2 Helices 6 and 7 are the most variable.

.

Small molecule docking

In order to examine the preference of allosteric ligands that are targeting the TSHR-TMD in either the dimeric or monomeric conformation, we examined the docking of a series of small molecules (n=46) some of which we have described earlier (33). Docking was performed as described earlier using the cluster sizes for monomer #1 [1141,289,570] and monomer #2 [791,923,346] to weight the docking scores of each ligand on the cluster representatives to give an overall docking score for each ligand; docking scores represent the free energy of binding to the receptor. **Supplementary Table 1**(30) shows the docking scores and the weighted averages of the scores for all 46 ligands. The weighted score averages over agonists and antagonists for the three targets (TRIO, Monomer #1 and Monomer#2) are shown in **Table 4**. This table also gives the separate averages for the agonist and antagonist groups of compounds found earlier to be biologically active or inactive. As there was very little difference between the respective active and inactive sets the table only shows the standard deviations for the whole agonist and antagonist sets. **Table 5** gives the results of the t-test comparing the agonist

and antagonist averages of docking scores against the three targets; statistically significant differences are shown in bold. These data show that certain small molecules have a significant preference for binding to one of the monomers compared to the other indicating that the difference between conformations is likely to be biologically significant.

The secondary structure elements (helices or loops) that formed contacts with ligands were also examined. **Table 6** shows the number of contacts between agonist and antagonist ligands for each helix and loop, separately for each monomer. As there are only 11 antagonists vs 35 agonists, the number of antagonists scaled by three is also shown to make the comparison fair. While there were significant differences between the agonist and antagonist docking scores, there was very little difference in the number of contacts. One exception would be Helix 5 that seems to be favored by agonists in both monomers. Also, Helix 4 was only contacted by a few ligands in monomer #2 – another indication of structural differences between the monomers in the dimer simulation.

DISCUSSION:

Dimerization is the normal state rather than the exception in many Class A and Class C G-protein coupled receptors (GPCR) (34,35). Homo or hetero dimerization in GPCRs appears to not only provide molecular mechanisms for agonist-induced activation but also increase specificity of ligand recognition and versatility of downstream signaling (36). Our earliest studies using native porcine thyroid membranes showed that TSHRs exist as higher order forms including

oligomeric and dimeric structures (5). Since then studies from our laboratory, and others (4,6,11,37), using biophysical techniques, including FRET and BRET, have developed important clarification of the existence of constitutive TSHR dimers and oligomeric forms in heterologous systems as well as native thyrocytes (6,8,38). Constitutive homodimeric and oligomeric TSHR forms have been shown to have a role in negative co-operativity (6,39), in regulating early events during receptor maturation and intracellular trafficking (9,40) and in $G_{\alpha q/11}$ signaling (37). We have previously also shown that these monomeric and higher order complexes are compartmentalized within lipid rafts in the plasma membrane and furthermore that these forms can bind TSH and TSHR autoantibodies (41) and may be regulated within lipid rafts (42,43). However, for understanding their exact roles under physiological or pathological conditions it is important to obtain better insight into the interaction caused by individual protomers that result in these higher order forms and conformations that may result due to these interactions. Although we have previous physical evidence of dimerization at the ectodomain and the TMD (8,11) the present in-silico study was designed to first examine just TMD dimerization using a membrane embedded model TMD which we developed earlier (16) and which mimics the native state of the TMD of the TSHR.

The DPPC membrane embedded monomeric TSHR-TMD model (**Figure 1a)** closely resembles the native receptor and was an ideal starting point for examining a dimeric structure. We obtained evidence for the tendency of the monomers to be held together as constitutive dimeric units (**Figures 1b & 1c**) seen in the animation of the 1000ns MD simulation trajectory as well as from the persistence of the contact residues in the dimeric interface which showed residue pairs in contact for more than 40% of the simulation time (**Figure 2**). Furthermore, the interface predicted by the Brownian

dynamics simulation approach was correct and the simulation showed subtle differences between the two monomers as well as between the conformations in the monomer and dimer simulations. These differences manifested themselves in the RMDSs of the superimposed structures and the hydrogen-bond patterns within the monomers (after excluding the hydrogen bonds within the helices). It is notable that there were only 11 hydrogen bonds that persisted in all three systems (out of the 87 described in **Supplementary Table 2**(30)). The variability in the dimeric interface further reinforced our earlier biochemical studies using truncated TMD constructs (11) and ECD beheaded constructs (9) suggesting the promiscuous nature of the dimerization interface. The cluster analysis and hydrogen bonding history (**Figures 3, 4 and 5**) within the monomers during the simulation further reveal flexibility of the conformation assumed by the monomers. This flexibility could be the cause of the asymmetric nature of dimerization leading to difficulty in obtaining cells solely expressing dimers to study their function in isolation. However, studies in other GPCRs, especially rhodopsin receptors, have revealed this dynamic intra- and inter- helical interactions which has been proposed from dimensional models obtained from atomic force microscope studies (44) and crystallization (45). Our MD simulations support and demonstrate the dynamic nature of the conformations that the monomers undergo as a dimeric unit which likely create novel conformations leading to the asymmetric interaction seen in TSHR-TMD dimerization.

In pursuit of developing novel therapeutics against the TSHR, our laboratory and others, have identified several agonists (7,31) and antagonists (46-48) for the TSHR. These are allosteric small molecules ligands (SMLs) targeted to binding pockets within the TSHR-TMD (49) and we used them as a tool to characterize the differences between the

conformations of the monomer during the MD simulation. Although there was little difference in the number of ligands contacting each helix and loop, statistical analysis of the docking scores (**Tables 5 & 6**) showed a clear difference between agonists and antagonists suggesting that small molecules which are structurally different but which go to similar binding pockets in the TSHR TMD can be influenced by the conformations of the monomers in the dimeric unit and may show preferential binding. Understanding the preference of the small molecules targeted to the receptor TMD will assist future SAR studies with the small molecules. It is known that small molecule ligands can enhance or disrupt dimerization/oligomerization of rhodopsin receptors (50) which also suggests that understanding TSHR dimerization will further our understanding of TSHR physiology

In conclusion this in silico study using a novel model of the TSHR TMD has provided further insight into our current understanding of TSH TMD dimerization and shown the dynamic nature of each monomeric unit that may lead to preferential binding of allosteric ligands.

Acknowledgments

This work was supported in part by NIH grant DK069713 & the VA Merit Award BX000800 (to TD), the Segal Family Fund and other generous anonymous donors and was also supported in part through the computational resources and staff expertise provided by the Department of Scientific Computing at the Icahn School of Medicine at Mount Sinai.

253

254
255

Table 1. Backbone RMSD between the cluster representatives of the two monomers and the TRIO model

	M1.1	M1.2	M1.3		M2.1	M2.2	M2.3		TRIO.1	TRIO.2	TRIO.3
M1.1	0.00	3.24	3.71		3.96	5.00	5.76		5.34	6.00	5.73
M1.2	3.24	0.00	2.67		4.82	5.56	6.30		5.46	5.96	5.72
M1.3	3.71	2.67	0.00		4.96	5.65	6.60		5.40	5.93	6.05
M2.1	3.96	4.82	4.96		0.00	3.49	4.90		4.49	5.25	5.13
M2.2	5.00	5.56	5.65		3.49	0.00	2.87		4.50	5.06	4.66
M2.3	5.76	6.30	6.60		4.90	2.87	0.00		5.39	5.86	5.16
TRIO.1	5.34	5.46	5.40		4.49	4.50	5.39		0.00	3.01	3.57
TRIO.2	6.00	5.96	5.93		5.25	5.06	5.86		3.01	0.00	3.21
TRIO.3	5.73	5.72	6.05		5.13	4.66	5.16		3.57	3.21	0.00

RMSDs are in Â. M1, M2 and TRIO indicate Monomer 1, Monomer 2 and TRIO (the monomer simulation), resp. The number after the period is the cluster number whose representative was used to calculate the RMSD.

Table 2. Significant hydrogen bonded residue pairs.

Res M1		Res M2				T %	M1 %	M2 %
ASP	3	LYS	8	H_1	H_1	35.6	23.0	33.7
SER	35	ASP	281	H_1	H_8	72.3	70.4	52.8
ASN	48	TRP	139	H_2	H_4	92.2	40.5	31.9
ASP	53	SER	264	H_2	H_7	83.0	95.6	35.8
MET	56	LEU	61	H_2	H_2	79.7	66.9	75.3
GLY	57	LEU	62	H_2	H_2	97.7	93.8	48.8
ASN	76	GLN	82	L_2-3	L_2-3	70.1	41.3	79.8
ALA	272	GLN	279	H_7	H_8	81.3	76.2	69.5
LEU	286	ILE	291	H_8	CTR	82.4	80.6	80.4
LEU	286	CYS	292	H_8	CTR	48.9	59.7	28.7
TYR	103	ILE	134	H_3	H_4	96.7	23.6	44.3

Residue pairs being hydrogen bonded more than 20% of the time in all three systems and being at least five residues apart are shown. Columns headed with T %, M1 % and M2 % give the percent of the time each residue pair was hydrogen bonded in the TRIO, Monomer 1 and Monomer 2, resp.

Table 3. Changes in helix length and radius.

	Helix #:	1		2		3		4		5		6.1		6.1		7.1		7.2		8	
M #1	Length	0.4	n	-1.8	S	0.6	n	-1.9	n	-0.8	S	-0.9	S	1.0	S	0.0	n	1.4	S	-0.1	n
	Radius	0.3	n	0.5	S	1.0	S	-1.3	n	-0.5	S	-0.4	S	0.4	S	0.4	S	0.4	S	0.2	n
M #2	Length	0.2	n	2.5	S	0.7	S	1.5	S	-0.6	n	-0.1	n	0.6	S	-0.3	n	1.8	S	-0.1	n
	Radius	0.3	n	1.3	S	0.5	n	0.3	n	-0.4	n	0.2	n	0.3	S	0.2	n	0.5	S	0.5	S

Changes were defined as the difference between the average of values from the representative structures and from the starting model structure.

A positive number indicates an increase with respect to the starting structure. The labels of the proline-separated segments of helices 6 and 7 have .1 and .2 added. The characters ‘S’ and ‘n’ indicate that the reference value is within or outside the range of the representative structure values, respectively

Table 4 - Docking scores for the small molecules initially designed as agonists and antagonists

SAMPLE	CALCULATED PARAMETER	TRIO	M1	M 2
Agonists (A) (#35):	Average (active)	-7.81	-8.44	-6.87
	Average(inactive)	-7.70	-8.41	-6.82
	Combined Average	-7.77	-8.43	-6.85
	SD	0.76	0.51	0.44
Antagonists (AA) (#11):	Average (active)	-7.62	-7.97	-6.82
	Average (inactive)	-8.44	-7.93	-6.68
	Combined Average	-7.62	-7.97	-6.82
	SD	1.20	0.65	0.76
All (#46):	Average	-7.84	-8.32	-6.92
	SD	0.88	0.58	0.52

The averages shown are averages over the weighted averages of the scores on the thre representative structures.

Table 5 - Two tailed Welch t-test results score averages

	A-TRIO	A-M1	A-M2	AA-TRIO	AA-M1	AA-M2	ALL-TRIO	ALL-M1	ALL-M2
A-TRIO									
A-M1	**<0.0001**								
A-M2	**<0.0001**	**<0.0001**							
AA-TRIO	0.7029	0.0521	0.0637						
AA-M1	0.4040	0.0497	**0.0001**	0.4084					
AA-M2	**0.0023**	**<0.0001**	0.9030	0.0802	**0.0012**				
ALL-TRIO	0.7025	**0.0003**	**<0.0001**	0.5776	0.5866	**0.0012**			
ALL-M1	**0.0007**	0.3678	**<0.0001**	0.0884	0.3500	**<0.0001**	**0.0028**		
ALL-M2	**<0.0001**	**<0.0001**	0.5142	0.0877	**0.0002**	0.6863	**<0.0001**	**<0.0001**	

Averages were calculated for agonists (A-) and antagonists (AA-) docked to the TMD models TRIO, Monomer #1 (M1) and Monomer #2 (M2), resp.

Table 6 – Number of contacts between the secondary structure elements of the TMD and the ~~angonist~~agonist (A) and antagonist (AA) ligands.

	Monomer #1			Monomer #2		
	AA	AA*3	A	AA	3*AA	A
Helix 2	3	9	26	0	0	2
Loop 2-3	102	306	301	14	42	57
Helix 3	49	147	153	13	39	19
Loop 4-5	167	501	586	279	837	985
Helix 4				23	69	85
Helix 5	1	3	12	17	41	72
Helix 6	18	54	52	5	15	12
Loop 6-7	49	147	122	44	132	91
Helix 7	49	147	180	3	9	15

Figure Legends

Figure 1: Cartoon representations of the initial monomer and dimer. a: Initial structure of TMD monomer, b: side view of the correctly oriented monomers protomers resulting in dimeric subunits. c: top view of b.
In the dimers, monomer 1 is tan and monomer 2 is orange; waters are represented as sticks.

Figure 2: History of residue pair contacts which involve atoms that are mutually proximal at the dimer interface more than 40% of the time.

Figure 3: 2D RMSD matrices for monomer 1 (panel a) and monomer 2 (panel b), sorted into clusters. The black lines delineate the clusters. The RMSD ranges for each color are specified under both matrices.

Figure 4: Cluster memberships for monomer 1 (panel a) and monomer 2 (panel b).

Figure 5: Hydrogen-bond history for monomer 2. Each line represents a residue pair; a line was broken for the time period when the residue pair was not hydrogen bonded. Residue numbers refer to the full TSHR.

Data availability: Original data generated and analyzed during this study are included in this published article or in the data repositories listed in References.

References

1. Davies TF, Andersen S, Latif R, Nagayama Y, Barbesino G, Brito M, Eckstein AK, Kahaly AS-GGJ. Graves' disease. *Nat Rev Dis Primers*. 2020;6:53.
2. Mizutori Y, Chen CR, McLachlan SM, Rapoport B. The thyrotropin receptor hinge region is not simply a scaffold for the leucine-rich domain but contributes to ligand binding and signal transduction. *Mol Endocrinol*. 2008;22:1171-1182.
3. Davies TF, Ando T, Lin RY, Tomer Y, Latif R. Thyrotropin receptor-associated diseases: from adenomata to Graves disease. *J Clin Invest*. 2005;115(8):1972-1983.
4. Latif R, Graves P, Davies TF. Ligand-dependent inhibition of oligomerization at the human thyrotropin receptor *J Biol Chem*. 2002;47:45059-45067.
5. Latif R, Graves P, Davies TF. Oligomerization of the human thyrotropin receptor: fluorescent protein-tagged hTSHR reveals post-translational complexes *J Biol Chem*. 2001;48:45217-45224.

6. Urizar E, Montanelli L, Loy T, Bonomi M, Swillens S, Gales C, Bouvier M, Smits G, Vassart G, Costagliola S. Glycoprotein hormone receptors: link between receptor homodimerization and negative cooperativity. *EMBO J*. 2005;24(11):1954-1964.

7. Latif R, Morshed SA, Ma R, Tokat B, Mezei M, Davies TF. A Gq Biased Small Molecule Active at the TSH Receptor. *Front Endocrinol*. 2020;11:372.

8. Latif R, Michalek K, Morshed SA, Davies TF. A tyrosine residue on the TSH receptor stabilizes multimer formation. *PLoS One*. 2010;26:e9449.

9. Latif R, Michalek K, Davies TF. Subunit interactions influence TSHR multimerization. *Mol Endocrinol*. 2010;24(10):2009-2018.

10. Cui M, Mezei M, Osman R. Modeling Dimerizations of Transmembrane Proteins using Brownian Dynamics Simulations. *Journal of Computer-Aided Molecular Design*. 2008;22:553-561.

11. Latif R, Ali MR, Mezei M, Davies TF. Transmembrane Domains of Attraction in the TSH Receptor. *Endocrinology*. 2014;156:488-489.

12. Ali MR, Latif R, Davies TF, Mezei M. Monte Carlo loop refinement and virtual screening of the thyroid-stimulating hormone receptor transmembrane domain. *Journal of Biomolecular Structure and Dynamics*. 2014:1-13.

13. Cui M, Mezei M, Osman R. Prediction of protein loop structures using a local move Monte Carlo approach and a grid-based force field. *Protein Eng Des Sel*. 2008;21:729-735.

14. Mezei M. Grand-Canonical Ensemble Monte Carlo Simulation of Dense Fluids: Lennard-Jones, Soft Spheres and Water. *Mol Phys*. 1987;61:565-582.

15. Mezei M. Erratum: Grand-canonical ensemble Monte Carlo study of dense liquid Lennard-Jones, soft spheres and water. *Molecular Physics*. 1989;67:1207-1208.

16. Mezei M, Latif R, Das B, Davies TF. Implications of an improved model of the TSH receptor transmembrane domain (TSHR-TMD -TRIO). *Endocrinology*. 2021;162:bqab051

17. Mezei M, Beveridge DL. Generic solvation sites in a crystal. *J Comp Chem*. 1984;6:523-527.

18. Mezei M. MMC: Monte Carlo program for molecular assemblies. URL: https://mezeim01.u.hpc.mssm.edu/mmc.

19. Humphrey W, Dalke A, Schulten K. VMD - Visual Molecular Dynamics. *J Molec Graphics*. 1996;14:33-38.

20. Jo S, Kim T, Iyer VG, Im W. CHARMM-GUI: a web-based graphical user interface for CHARMM. *J Comput Chem*. 2008;29(11):1859-1865.

21. Emilia L. Wu, § Xi Cheng,1,§ Sunhwan Jo,1,§ Huan Rui,1,§ Kevin C. Song,1,§ Eder M. Dávila-Contreras,1 Yifei Qi,1 Jumin Lee,1 Viviana Monje-Galvan,2 Richard M. Venable,3 Jeffery B. Klauda,2,* and Wonpil Im. CHARMM-GUI Membrane Builder Toward Realistic Biological Membrane Simulations. *J Comput Chem*. 2014;35:1997–2004.

22. Phillips JC, Braun R, Wang W, Gumbart J, Tajkhorshid E, Villa E, Chipot C, Skeel RD, Kale L, Schulten K. Scalable molecular dynamics with NAMD. *J Comput Chem*. 2005;26(16):1781-1802.

23. Kaufman L, Rousseeuw PJ. "Clustering by means of Medoids". Statistical Data Analysis Based on the L1–Norm and Related Methods. North-Holland.

24. Mezei M. Simulaid: a simulation facilitator and analysis program. *J Comput Chem*. 2010;31(14):2658-2668.

25. Mezei M, Filizola M. TRAJELIX: A computational Tool for the Geometric Characterization of Protein Helices During Molecular Dynamics Simulations. *J Computer-Aided Molecular Design*. 2006;20:97-107.

26. Induced Fit Docking protocol 2015-2, Glide version 6.4, Prime version 3.7. New York, NY, 2015: Schrödinger, LLC.

27. Friesner RA, Banks JL, Murphy RB, Halgren TA, Klicic JJ, Mainz DT, Repasky MP, Knoll EH, Shaw DE, Shelley M, Perry JK, Francis P, Shenkin PS. Glide: A New Approach for Rapid, Accurate Docking and Scoring. 1. Method and Assessment of Docking Accuracy. *J Med Chem,*. 2004;47: 1739–1749.

28. Lee MS, Jr. FRS, III CLB. Novel generalized Born methods. *J Chem Phys* 2002;116:10606

29. Brooks BR, Bruccoleri RE, Olafson BD, States DJ, Swaminathan S, Karplus M. CHARMM: A program for macromolecular energy, minimization and dynamics calculation. *J Comp Chem*. 1983;4:187 –217.

30. M. Mezei RL, B. Das, & T.F. Davies. Supplementary material for "Modeling TSH Receptor Dimerization at the Transmembrane Domain". *Endocrinology* 2022.
URL: https://figshare.com/articles/dataset/TSHR_dim_supplement_pdf/21191512

31. Latif R, Ali MR, Ma R, David M, Morshed SA, Felsenfeld DP, Ohlmeyer M, Lau W, Mezei M, Davies TF. New small molecule agonists to the thyrotropin receptor. *Thyroid*. 2015;25:51-62.

436 32. Mezei M, Zhou MM. Dockres: a computer program that analyzes the output of virtual screening of small molecules.
437 *Source Code Biol Med*. 2010;5:2.
438 33. Latif R, Davies TF. Targeting the thyroid-stimulating hormone receptor with small molecule ligands and antibodies.
439 *Expert Opinion on Therapeutic Targets*. 2015;19:835-847.
440 34. Faron-Górecka A, Szlachta M, Kolasa M, Solich J, Górecki A, Kuśmider M, DariuszŻurawek, Dziedzicka-
441 Wasylewska M. Understanding GPCR dimerization. In: Shukla AK, ed. Vol 149: Elsevier; 2019:155-178.
442 35. Gurevich VV, Gurevich EV. How and why do GPCRs dimerize? *Trends in Pharmacological Sciences*. 2008;29:234-
443 240.
444 36. Breitwieser GE. G Protein–Coupled Receptor Oligomerization. *Circulation Research*. 2004;94:17-27.
445 37. Allen MD, Neumann S, Gershengorn MC. Occupancy of both sites on the thyrotropin (TSH) receptor dimer is
446 necessary for phosphoinositide signaling. *FASEB J*. 2011;25(10):3687-3694.
447 38. Graves PN, Vlase H, Bobovnikova Y, Davies TF. Multimeric complex formation by the thyrotropin receptor in
448 solubilized thyroid membranes. *Endocrinology*. 1996;276:45217-45224.
449 39. Chazenbalk GD, Kakinuma A, Jaume JC, McLachlan SM, Rapoport B. Evidence for negative cooperativity among
450 human thyrotropin receptors overexpressed in mammalian cells. *Endocrinology*. 1996;137(11):4586-4591.

40. Calebiro D, de Filippis T, Lucchi S, Covino C, Panigone S, Beck-Peccoz P, Dunlap D, Persani L. Intracellular entrapment of wild-type TSH receptor by oligomerization with mutants linked to dominant TSH resistance. *Hum Mol Genet*. 2005;14(20):2991-3002.

41. Graves PN, Vlase H, Davies TF. Folding of the recombinant human thyrotropin (TSH) receptor extracellular domain: identification of folded monomeric and tetrameric complexes that bind TSH receptor autoantibodies. *Endocrinology*. 1995;136(2):521-527.

42. Latif R, Ando T, Davies TF. Lipid rafts are triage centers for multimeric and monomeric thyrotropin receptor regulation. *Endocrinology*. 2007;148(7):3164-3175.

43. Latif R, Graves P, Davies TF. Ligand-dependent inhibition of oligomerization at the human thyrotropin receptor. *J Biol Chem*. 2002;277(47):45059-45067.

44. Fotiadis D, Jastrzebska B, Philippsen A, Müller DJ, Palczewski K, Engel A. Structure of the rhodopsin dimer: a working model for G-protein-coupled receptors. *Current Opinion in Structural Biology*. 2006;16:252-259.

45. Zhao DY, Pöge M, Morizumi T, Gulati S, Eps NV, Zhang J, Miszta P, Filipek S, Mahamid J, Plitzko JM, Baumeister W, Ernst OP, Palczewski K. Cryo-EM structure of the native rhodopsin dimer in nanodiscs. *J Biol Chem*. 2019;294:14215-14230.

46. Neumann S, Huang W, Titus S, Krause G, Kleinau G, Alberobello AT, Zheng W, Southall NT, Inglese J, Austin CP, Celi FS, Gavrilova O, Thomas CJ, Raaka BM, Gershengorn MC. Small-molecule agonists for the thyrotropin receptor stimulate thyroid function in human thyrocytes and mice. *PNAS*. 2009;106:12471-12476.

47. S.Neumann, M.C.Gershengorn. Small molecule TSHR agonists and antagonists Le récepteur de TSH et les petites molécules : les agonistes et les antagonistes. *Annales d'Endocrinologie*. 2011;72:74-76.

48. Latif R, Realubit RB, Karan C, Mezei M, Davies TF. TSH Receptor Signaling Abrogation by a Novel Small Molecule. *Frontiers in Endocrinology*. 2016;7:130.

49. Kleinau G, Haas A-K, Neumann S, Worth CL, Hoyer I, Furkert J, Rutz C, Gershengorn MC, Schülein R, Krause G. Signaling-sensitive amino acids surround the allosteric ligand binding site of the thyrotropin receptor. *The FASEB Journal*. 2010;24:2347–2354.

50. Getter T, Kemp A, Vinberg F, Palczewski K. Identification of small-molecule allosteric modulators that act as enhancers/disrupters of rhodopsin oligomerization. *Jounal of Biological Chemistry*. 2021;297.

Figure 1

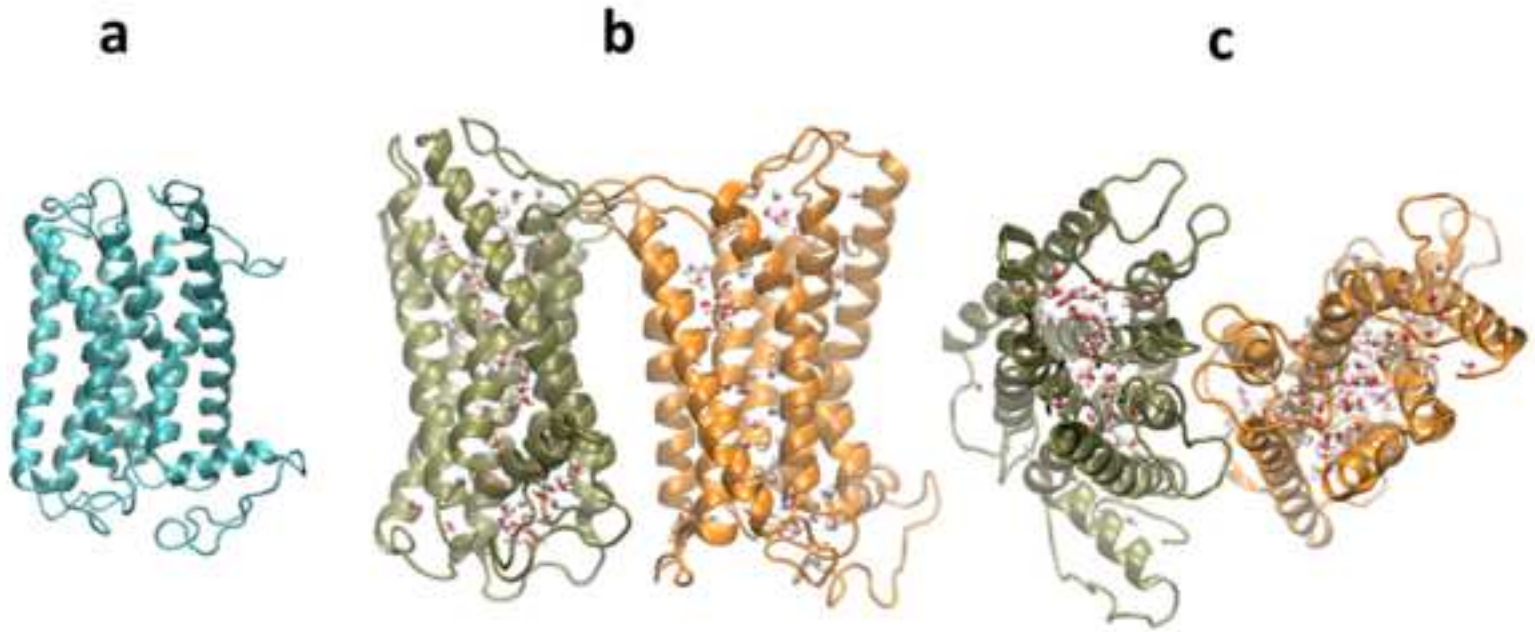

Figure 2

Click here to access/download;Figure;fig_2.epi

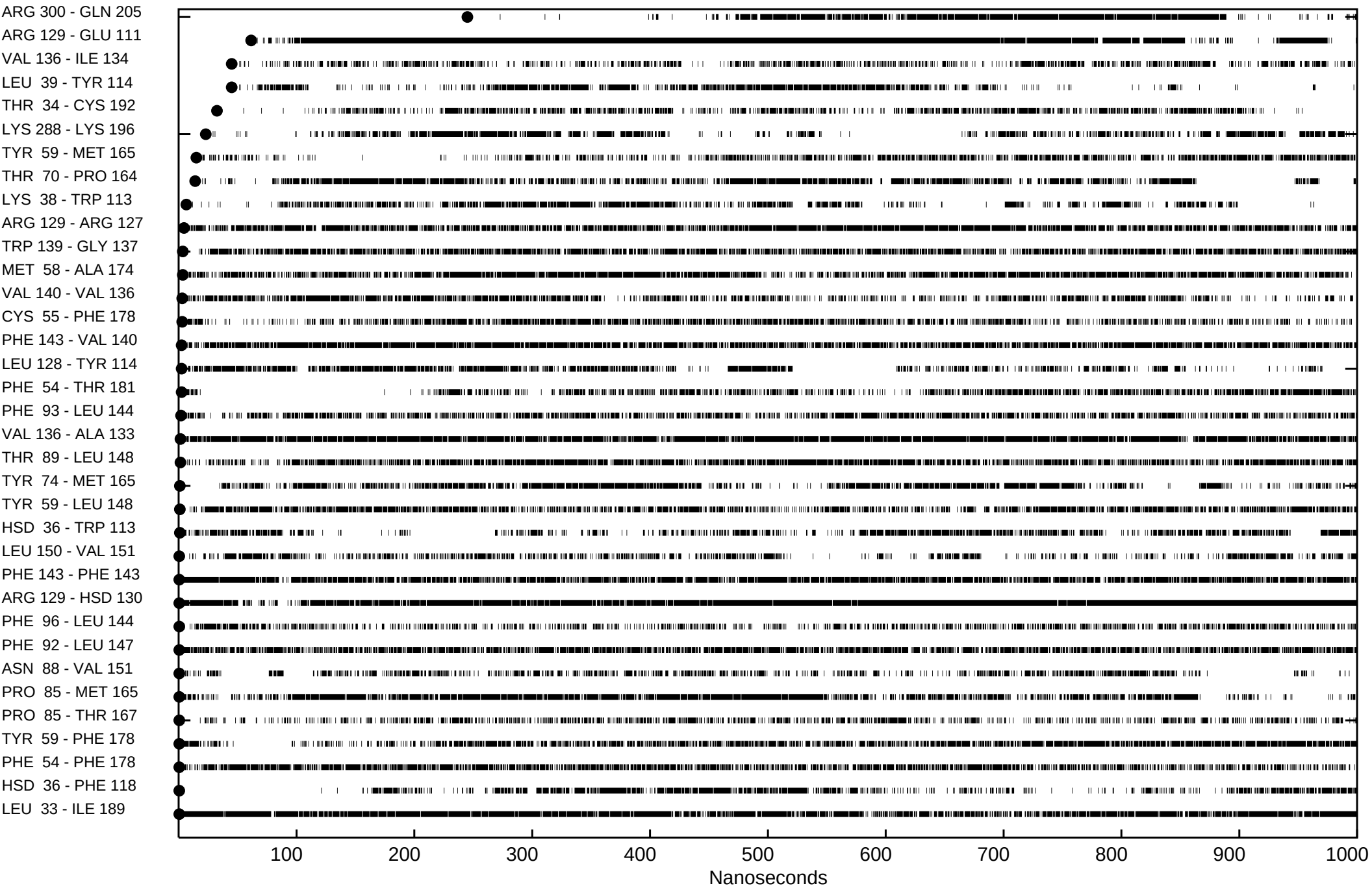

Figure 3

Click here to access/download;Figure;fig_3ab.epi

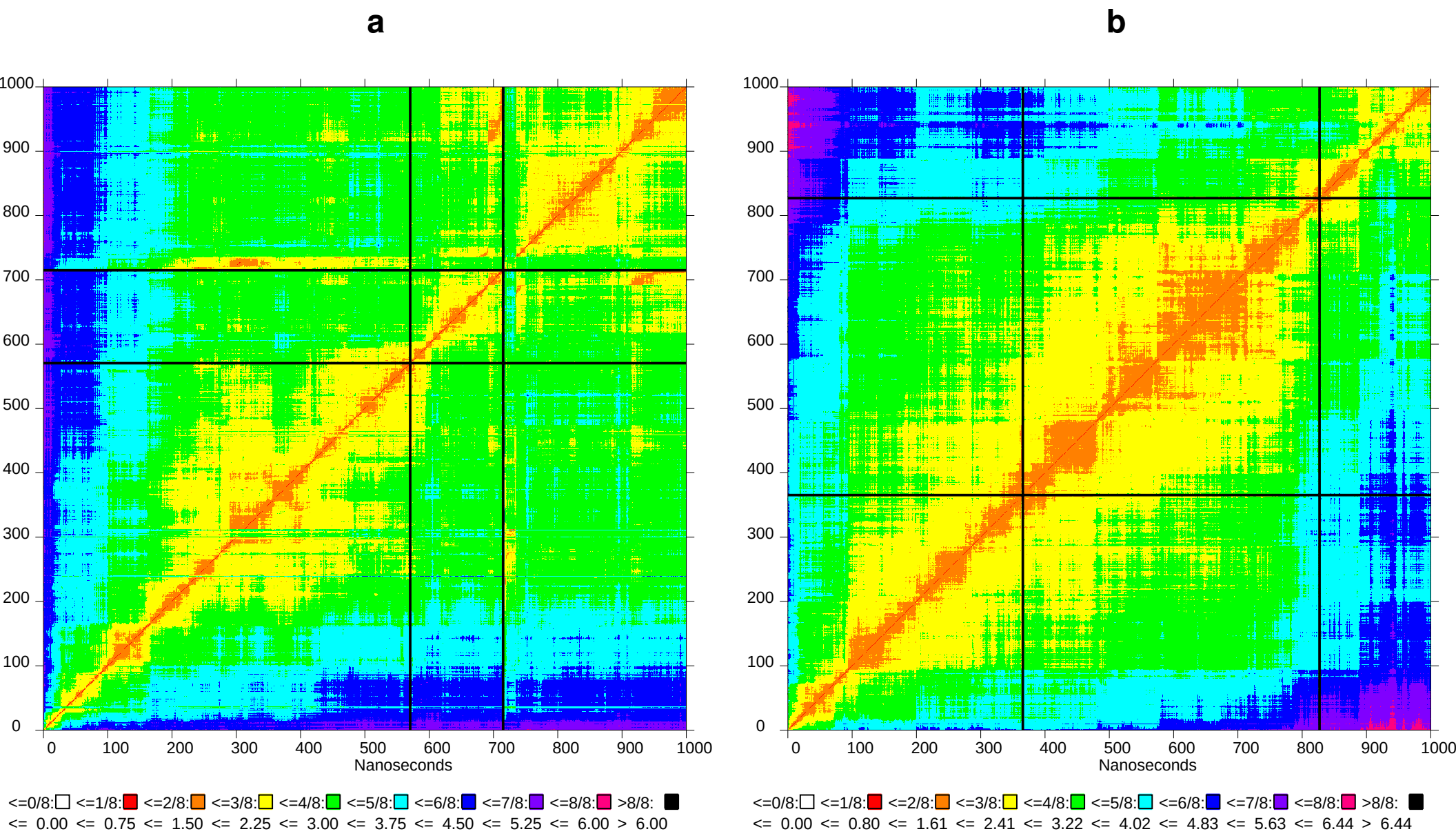

Figure 4

Click here to access/download;Figure;fig_4ab.epi

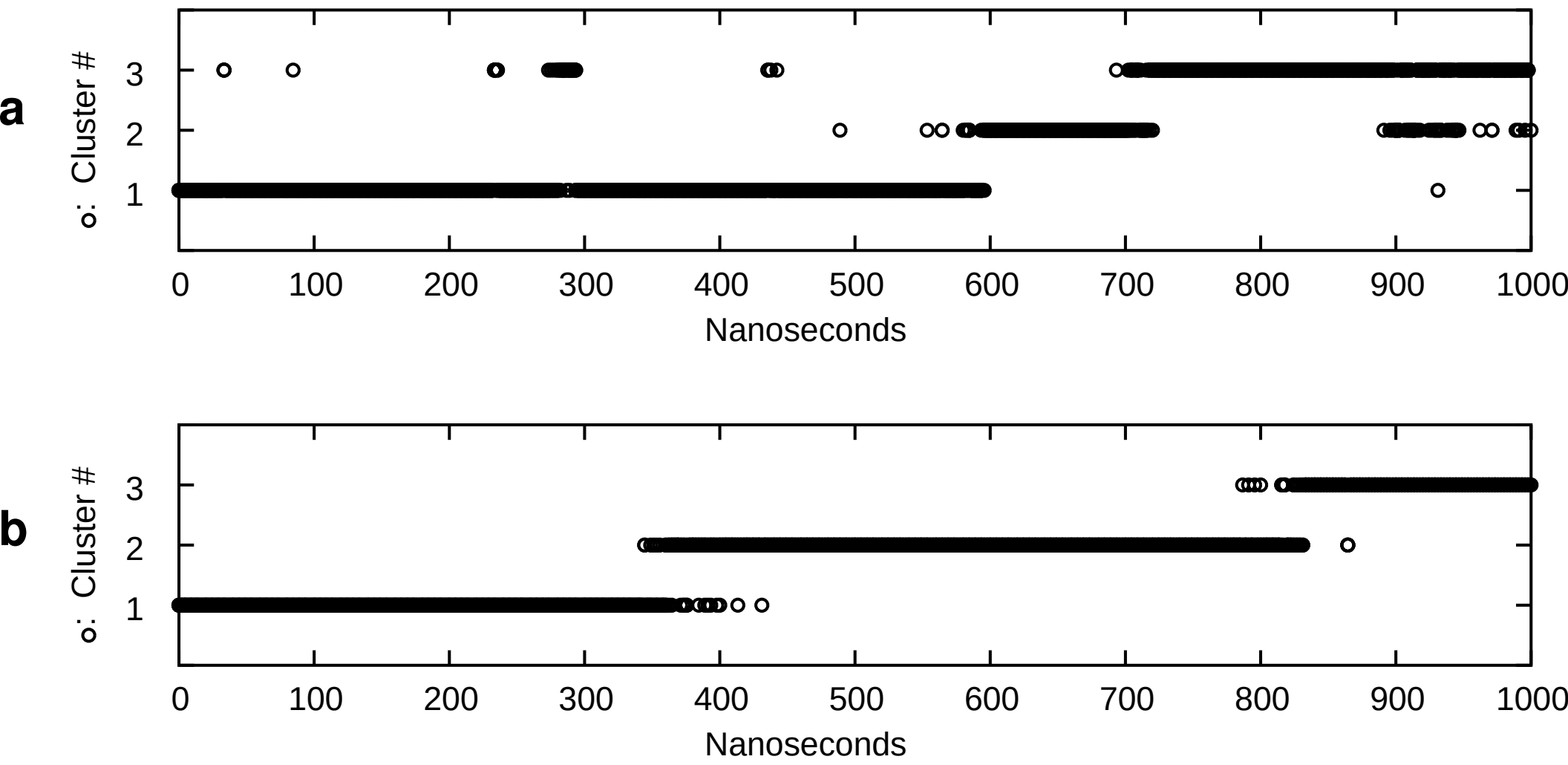

Figure 5

Click here to access/download;Figure;fig_5.epi